OpenSkinFrictionFromGLOF: An Open Source Program for Extraction of Skin Friction Fields from Global Luminescent Oil-Film Images

Tianshu Liu*, David M. Salazar

Department of Mechanical and Aerospace Engineering

Western Michigan University, Kalamazoo, MI 49008

(02/02/2023)

(Submitted to Journal of Open Research Software for consideration of publication)

*: Corresponding author

Department of Mechanical and Aerospace Engineering, G-217, Parkview Campus, Western Michigan University, Kalamazoo, MI 49008, USA

tianshu.liu@wmich.edu, 269-276-3426

Abstract

This paper describes "OpenSkinFrictionFromGLOF", an open source program in Matlab for extraction of high-resolution skin friction fields from global luminescent oil-film (GLOF) images. This program is a useful tool for researchers to apply the GLOF method to complex separated flows. The principles of the GLOF method are concisely described, including the projected thin-oil-film equation that is re-cast to the physics-based optical flow equation, the variational solution, an error analysis, and averaging of snapshot solutions. The central part of this paper is the descriptions of the main program, relevant subroutines and selection of the relevant parameters in GLOF computation. An example of the square junction flow is given to demonstrate the applications of the GLOF method.

Keywords: skin friction, global luminescent oil-film, optical flow, variational solution, flow visualization, fluid mechanics, measurement technique, image processing, Matlab

(1) Overview

Introduction

The global luminescent oil-film (GLOF) method was developed by Liu et al. [1] for extraction of high-resolution skin friction fields from GLOF images. The GLOF method has been applied to various complex flows [2-12]. The GLOF method is based on oil-film thickness measurement and then skin friction is inferred from the temporal-spatial evolution of the oil-film thickness. To visualize the evolution of the oil-film development, luminescent oil is used since the oil-film thickness is proportional to the luminescent emission intensity when the oil is optically thin. In experiments, a thin luminescent oil film is brushed or sprayed on a surface in a

region of interest before starting a wind tunnel, and it is illuminated by light sources with a suitable wavelength such as ultraviolet (UV) lights. Therefore, oil-film thickness measurement is converted to luminescent intensity measurement by using a camera with a suitable optical filter. After flow is turned on, a time sequence of evolving GLOF images is acquired. From a standpoint of image processing, the foundation for application of the GLOF method is the thin-oil-film equation projected onto the image plane, which can be re-cast to the optical flow equation for the luminescent intensity (proportional to the image intensity) where the optical flow is interpreted as the normalized skin friction. This optical flow equation has the same form as the physics-based optical flow equation derived by Liu and Shen [12] for various flow visualizations. Therefore, the GLOF method uses the open-source optical flow algorithm "OpenOpticalFlow" to determine a snapshot skin friction field from a pair of sequential GLOF images [13]. Further, a normalized time-averaged skin friction field is obtained by averaging a a sequence of snapshot solutions.

The objective of this paper is to describe an open-source program in Matlab for extraction of high-resolution skin friction fields from a sequence of GLOF images. First, the principles of the GLOF method are briefly described, including the projected thin-oil-film equation, the variational method, a short error analysis, and averaging of snapshot solutions. Then, the main program and the key subroutines are described, particularly on the selection of the relevant parameters in optical flow computation. Next, to demonstrate the applications of this program, several examples based on GLOF images are presented.

Principles of the GLOF method

a. Projected thin-oil-film equation

The GLOF method is based on luminescent-oil-thin thickness measurement and the solution of the projected thin-oil-film equation as an inverse problem. For an optically thin luminescent oil film applied to a surface under suitable illumination, the oil-film thickness h is proportional to the normalized luminescent intensity, i.e., $h = \beta^{-1}(I / I_{ex})$, where I is the luminescent intensity, I_{ex} is the intensity of the illumination light on the surface, and β is a coefficient proportional to the quantum efficiency of luminescent dye seeded in the oil. We consider an orthographic projection transformation between the surface coordinates (X_1, X_2) in the object space and the image coordinates (x_1, x_2), i.e., $\partial / \partial X_i = \lambda \partial / \partial x_i$, where λ is a scaling constant that is approximately a ratio between the focal length of a camera/lens system and its distance to the surface. Define the normalized luminescent intensity $g = I / I_{ex}$ as a measurable quantity that eliminates the effect of non-uniform illumination.

Replacing h by I in the thin-oil-film equation and using the orthographic projection transformation, we obtain the following equation

$$\frac{\partial g}{\partial t} + \nabla \cdot (g \hat{\boldsymbol{\tau}}) = f , \tag{1}$$

where $\hat{\boldsymbol{\tau}} = \boldsymbol{\tau}\, g\, (\lambda / 2\mu_o \beta)$ is an equivalent skin friction vector, and $\boldsymbol{\tau} = (\tau_1, \tau_2)$ is a skin friction vector projected onto the image plane (x_1, x_2), and $\nabla = \partial / \partial x_i$ $(i = 1, 2)$ is the gradient operator. The right-hand-side (RHS) term in Eq. (1) is defined as

$$f = \lambda \nabla \cdot \left[\left(\lambda \nabla p - \rho_o \boldsymbol{a} \right) \frac{g^3}{3\mu_o \beta^2} \right], \tag{2}$$

where μ_o is the oil viscosity, ρ_o is the oil density, and $\boldsymbol{a}$ is the gravity vector. The term f represents the effects of the pressure gradient and gravity, which is in the order of $\lambda h^3 << 0$ since $\lambda << 0$ and $h^3 << 0$. Therefore, this term is considered as a higher-order small term in Eq. (3). Interestingly, Eq. (1) has the same form of the physics-based optical flow equation for

various flow visualizations [13]. Therefore, the same optical flow problem can be solved to determine a skin friction field.

b. Variational solution

Solving the single equation, Eq. (1), for the two unknown components $\hat{\boldsymbol{\tau}} = (\hat{\tau}_1, \hat{\tau}_2)$ is a typical inverse problem, in which additional constraint is required for a unique solution. Therefore, a variational method is used for solving this problem. We consider a functional with a smoothness regularization term on an image domain D, which is defined as

$$J(\hat{\boldsymbol{\tau}}) = \int_D \left(\frac{\partial g}{\partial t} + \nabla \cdot (g \hat{\boldsymbol{\tau}}) - f \right)^2 dx_1 dx_2 + \alpha \int_D \left(\left| \nabla \hat{\tau}_1 \right|^2 + \left| \nabla \hat{\tau}_2 \right|^2 \right) dx_1 dx_2 , \tag{3}$$

where α is a Lagrange multiplier. The minimization of $J(\hat{\boldsymbol{\tau}})$ leads to the Euler-Lagrange equations, i.e.,

$$g \nabla \left[\frac{\partial g}{\partial t} + \nabla \cdot (g \hat{\boldsymbol{\tau}}) - f \right] + \alpha \nabla^2 \hat{\boldsymbol{\tau}} = 0 , \tag{4}$$

where $\nabla^2 = \partial^2 / \partial x_i \partial x_i$ $(i = 1,2)$ is the Laplace operator. The Neumann condition $\partial \hat{\boldsymbol{\tau}} / \partial n = 0$ is imposed on an image domain boundary ∂D. The standard finite difference method is used to solve Eq. (4) with the Neumann condition $\partial \hat{\boldsymbol{\tau}} / \partial n = \boldsymbol{0}$ [13, 14]. The numerical solution of Eq. (4) gives the equivalent skin friction $\hat{\boldsymbol{\tau}}$ and thus the relative projected skin friction vector $\hat{\boldsymbol{\tau}} / g$ is obtained. The Lagrange multiplier plays a role in controlling the diffusion term in Eq. (4). As a rule of thumb, a sufficiently small value of α is selected to preserve sharp features as long as a numerical solution of Eq. (4) converges. Selection of a suitable value of α can be made based on simulations on synthetic images. When GLOF images contain rich features with sufficiently

large intensity gradient, a solution of Eq. (4) is not sensitive to the Lagrange multiplier in a considerable range of α.

c. Errors

In an error analysis, the image intensity and skin friction vector are decomposed into a basic solution and an error, i.e., $g = g_0 + \delta g$ and $\hat{\boldsymbol{\tau}} = \hat{\boldsymbol{\tau}}_0 + \delta\hat{\boldsymbol{\tau}}$, where g_0 and $\hat{\boldsymbol{\tau}}_0$ satisfy exactly Eq. (4), and $\delta\hat{\boldsymbol{\tau}}$ is the resulting error in skin friction and δg is an error in the luminescence measurements. Substitution of the above decompositions into Eq. (4) leads to an error propagation equation and then a formal estimate of the relative error

$$\frac{(\delta\hat{\boldsymbol{\tau}})_N}{\|\hat{\boldsymbol{\tau}}_0\|} = \frac{\delta t\, g_{tt}}{2\|\nabla g_0\|_{char}\|\hat{\boldsymbol{\tau}}_0\|} - \frac{\alpha}{g_{I0}\|\nabla g_0\|_{char}}\nabla^{-1}\left\{\nabla^2\left[\frac{(\delta\hat{\boldsymbol{\tau}})_N}{\|\hat{\boldsymbol{\tau}}_0\|}\right]\right\}, \tag{5}$$

where $(\delta\hat{\boldsymbol{\tau}})_N = \delta\hat{\boldsymbol{\tau}}\cdot\boldsymbol{N}_T$ is the projected skin friction error along the unit normal vector $\boldsymbol{N}_T = \nabla g_0 / \|\nabla g_0\|$, $g_{tt} = \partial^2 g_0 / \partial t^2$ is the second-order time derivative, δt is a time step between two consecutive images, $\|\nabla g_0\|_{char}$ is a characteristic intensity gradient magnitude, and $\|\hat{\boldsymbol{\tau}}_0\|$ is a characteristic value of skin friction (e.g. the mean value). The symbol ∇^{-1} in Eq. (5) is a symbolic inverse operator for the solution of the partial differential equation $\nabla\phi = \boldsymbol{b}$.

The first term in the RHS in Eq. (5) represents an elemental error in the time differentiation. Since δt and $\|\nabla g_0\|_{char}$ are finite, a constraint is $\delta t\|\nabla g_0\|_{char}^{-1} \geq d$, where d is a small positive constant, Therefore, a finite skin friction error $\delta\hat{\boldsymbol{\tau}}$ always exists, which imposes an ultimate limitation on the accuracy of extracting skin friction from GLOF images. For a given time step δt, larger intensity gradient leads to a smaller skin friction error. Rich local

features with large intensity gradient in GLOF images ensure the accuracy in computations. The second term in the RHS in Eq. (5) represents the effect of the Lagrange multiplier, which is proportional to is $\alpha\|\nabla g_0\|_{char}^{-1}$. Therefore, when $\|\nabla g_0\|_{char}$ is small, the Lagrange multiplier α must be small to reduce the error.

d. Averaging of snapshot solutions

Development of a luminescent oil film on a surface is time-dependent even in steady flow. The numerical solution of Eq. (4) gives a snapshot skin friction field from a pair of successive images. From a time sequence of GLOF images, a series of snapshot solutions at successive moments are obtained. Physically speaking, a snapshot solution captures salient skin friction signatures in regions where the oil-film evolution is more sensitive to flow at that moment. Therefore, a time sequence of snapshot solutions is required to capture major skin friction signatures at different moments during the oil-film evolution process. To reconstruct a relative steady-state or time-averaged skin friction field, snapshot solutions are superposed or averaged. In general, by using the GLOF method, a normalized skin friction field is given without in-situ calibration. An absolute skin friction field can be obtained by in-situ calibration that utilizes some accurate values of skin friction at several reference locations (at least one) given by reliable techniques like an interferometric oil-film skin friction meter or computational and theoretical methods.

Implementation and architecture

a. General description

The program package “OpenSkinFrictionFromGLOF” is written in Matlab, and the files are contained in a folder named “OpenSkinFrictionFromGLOF.v1” in the GitHub site: XXX. The main program is “GLOF_Diagnostics_Run.m”. The central part is the optical flow computation using the subroutine “snapshot_solution_fun” that calls a subroutine “OpticalFlowPhysics_fun”. This optical flow subroutine is essentially the same as the open-source program “OpenOpticalFlow” described by Liu [15], which uses the Horn-Schunck estimator (“horn_schunck_estimator.m”) and the Liu-Shen estimator (“liu_shen_estimator.m”). In “GLOF_Diagnostics_Run.m”, a sequence of GLOF images is loaded and the snapshot solutions of skin friction are obtained by using the optical flow method for selected pairs of GLOF images. Then, a relative (normalized) skin friction field is reconstructed by averaging the snapshot solutions. In addition, some pre-processing can be made such image filtering for removing random noise, image masking, and image downsampling.

The input parameters are the same as those in “OpenOpticalFlow”. A pair of GLOF images is denoted by “Im1” and “Im2” that could be in the conventional image format such as “tif”, “bmp”, or “jpeg”. The timestep between “Im1” and “Im2” should be suitably selected depending on the sequence of images at a frame rate. In general, for optical flow computation, a typical displacement between “Im1” and “Im2” is less than 5 pixels, which can be control by image downsampling. The timestep between two snapshot solutions and the total number of snapshot solutions for averaging (superposition) should be selected to cover the evolution of the oil-film. “lambda_1” is the Lagrange multiplier for the Horn-Schunck estimator for initial estimation, and “lambda_2” is the Lagranger multiplier for the Liu-Shen estimator for refined estimation. “size_filter” is the Gausian filter size for removing random noise in images in pixels. For operational simplicity, other parameters such as “index_masking” and “index_masking” are

fixed. The optical flow processing can be made in a selected rectangular domain of interest for regional flow diagnostics when the index "index_region" is set at 1. Otherwise, the processing is conducted in the whole image domain when the index "index_region" is set at 0.

b. The Lagrange multiplier

The optical flow program uses the Horn-Schunck estimator ("horn_schunck_estimator.m") for an initial solution and Liu-Shen estimator ("liu_shen_estimator.m") for a refined solution of Eq. (4). In the main program, the Lagrange multipliers "lambda_1" and "lambda_2" are selected for the Horn-Schunck and Liu-Shen estimators, respectively. For example, "lambda_1" = 20 and "lambda_2" = 2000 for typical optical flow computations.

There is no rigorous theory for determining the Lagrange multiplier in the variational formulation of the optical flow equation. The Lagrange multiplier acts like a diffusion coefficient in the corresponding Euler-Lagrange equations. Therefore, a larger Lagrange multiplier tends to smooth out finer flow structures. In general, the smallest Lagrange multiplier that still leads to a well-posed solution could be selected by a trial-and-error process. However, within a considerable range of the Lagrange multipliers, the solution is not significantly sensitive to its selection. Simulations based on a synthetic velocity field for a specific measurement could be carried out to determine the Lagrange multiplier by using an optimization scheme [8].

c. Filtering

Pre-processing of images is sometimes required to remove the random noise by using a Gaussian filter. The standard deviation (std) of a Gaussian filter is selected, depending on the noise level in a specific application (for example the std of a Gaussian filter is 4-6 pixels for

images of 480×520 pixels). In the main program, the mask size of a Gaussian filter is given by the parameter called "size_filter", and the std of the Gaussian filter is 0.6 of the mask size.

Example: junction flows

Experimental setup and conditions

The GLOF meter is applied to junction flows to obtain high-resolution skin friction fields around cylinders on the flat-plate surface. Figure 1 shows a typical setup for GLOF visualization on a flat plate in junction flows. Measurements were made on a 3.2-mm thick aluminum flat plate with a round leading edge in a low-speed wind tunnel with a 0.406-m×0.406-m test section. A cylinder (a circular, square or diamond cylinder) was vertically mounted on the flat plate at $x = 241\ mm$ from the flat-plate leading edge. The freestream velocity was 20 m/s. The local reference Reynolds number was $Re_x = U_\infty x_{ref} / \nu_a = 2.14 \times 10^5$, where $x_{ref} = 168\ mm$ is a reference location from the flat-plate leading edge before boundary-layer separation and ν_a is the kinematical viscosity of air. Since the freestream turbulent intensity in the wind tunnel was about 1%, $Re_x = 2.14 \times 10^5$ was lower than the empirical critical Reynolds numbers $Re_{x,cri} \approx 2.8 \times 10^5$ for flat-plate boundary-layer transition on a flat plate, the incoming boundary layer was supposed to be laminar before separation. Luminescent oil-film visualization was also applied to the region near the flat-plate leading edge, and no flow transition and separation bubble was found. The estimated momentum, displacement and boundary layer thicknesses based on the flat-plate laminar boundary-layer solution were 0.22, 0.75 and 1.67 mm, respectively. The Reynolds number based on the displacement thickness was $Re_{\delta^*} = U_\infty \delta^* / \nu_a = 1013$, where $\delta^* = 0.75mm$ is the displacement thickness.

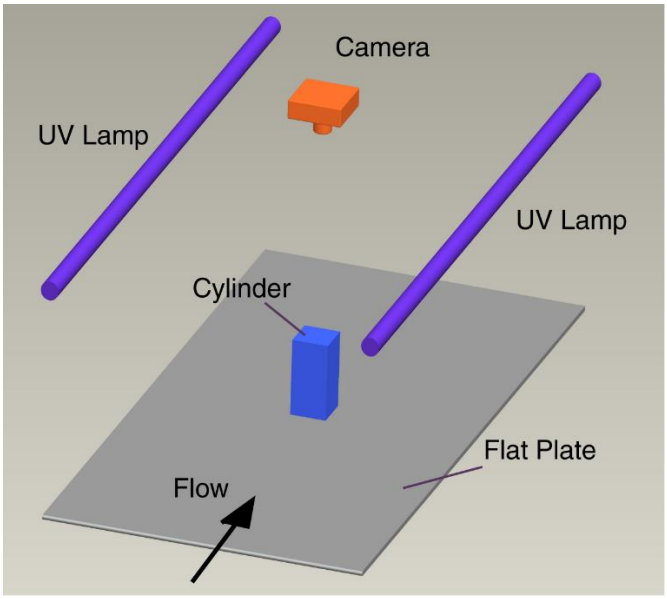

Figure 1. Illustration of the experimental setup for luminescent oil-film visualization in junction flows.

To make luminescent oil, a small amount of oil-based UV dye (Petroleum Tracer Concentrate DFSB-K175 from Risk Reactor, www.riskreactor.com) was mixed with Dow Corning silicone oil with the viscosity of 200 cs. The resulting luminescent oil emitted the radiation at a wavelength of about 590 nm when it was illuminated by UV lamps. A white Mylar sheet covered on the measurement area for enhancing the luminescent emission. The UV lamps were arranged to ensure a uniform illumination field in the area of interest. A 550-nm long-pass filter was used to filter the light captured by a camera allowing only detection of the luminescent emission. Before turning on the tunnel, the luminescent oil was brushed on the surface. After the flow was turned on, the luminescent oil evolution was recorded at 25 f/s using an 8-bit CMOS camera viewing perpendicularly the flat-plate surface.

Square cylinder

GLOF diagnostics was also conducted on the flat plate around a square cylinder with a 51-mm×51-mm cross-section and a 121-mm height in the junction flow in the same flow conditions as those in the case of the circular cylinder. The ratio between the incoming boundary-layer thickness and the equivalent diameter was 0.03 and the Reynolds number based on the equivalent diameter was 7.3×10^4, where the equivalent diameter is $D=\sqrt{4S_{sq}/\pi}=57.5\ mm$ and S_{sq} is the cross-section area of the square cylinder. Figure 2 shows a typical pair of GLOF images. Figure 3 shows the time-averaged skin friction field extracted by the GLOF method in the square junction flow: skin friction vectors and skin friction lines. The spatial resolution of the extracted skin friction field is one vector per pixel. The separation and attachment lines associated with the horseshoe vortex around the square cylinder are clearly identified.

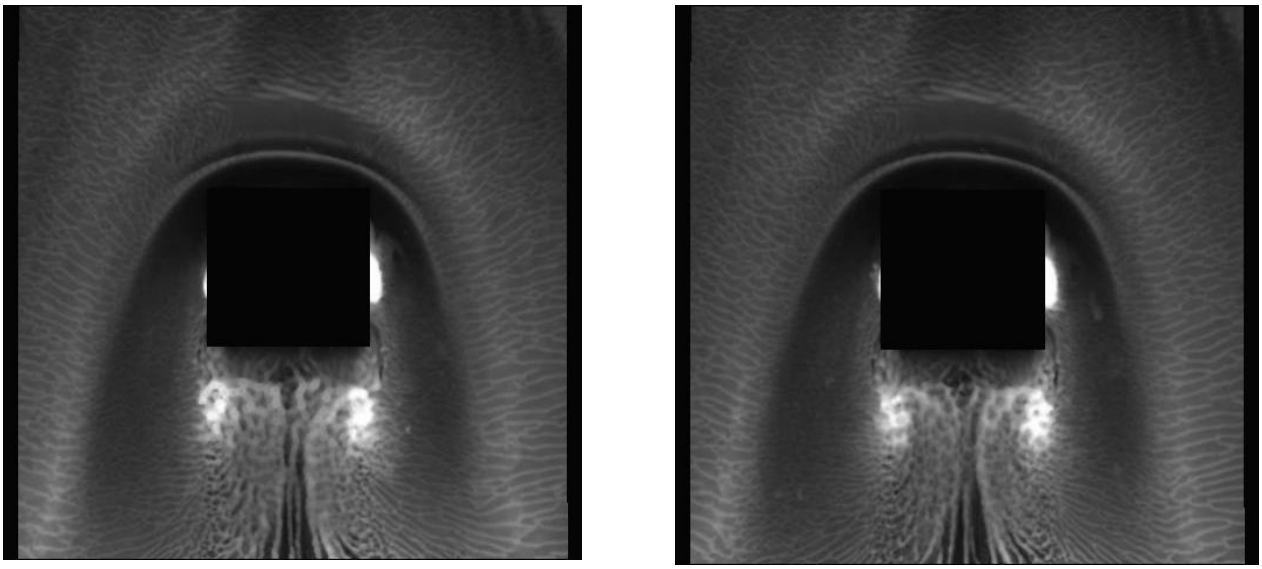

(a) (b)

Figure 2. A typical pair of GLOF images in the square junction flow.

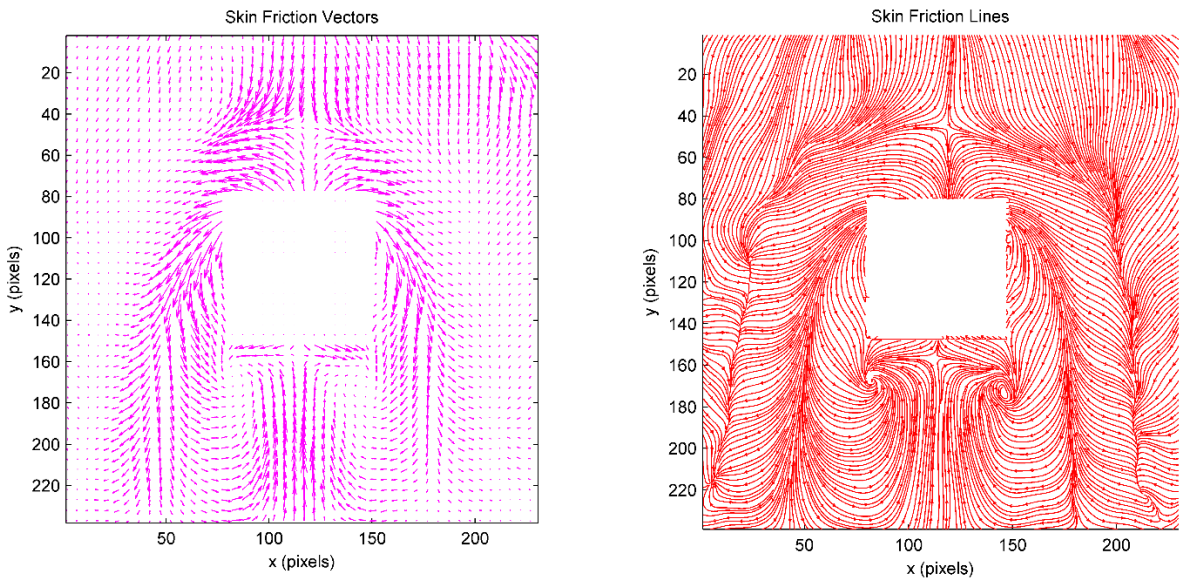

(a) (b)

Figure 3. The time-averaged skin friction field extracted by the GLOF method in the square junction flow: (a) skin friction vectors, and skin friction lines.

The extracted high-resolution skin friction field allows a topological analysis of critical points, and separation and attachment lines. Figure 4 shows the skin friction topology in the square junction flow obtained by Liu et al. using the GLOF method [XX]. The primary separation line associated with the horseshoe vortex in the front of the cylinder is originated from the saddle S_1. The primary spiraling nodes N_1 and N_2 connected through the saddle S_2 occur behind the square cylinder. Additional finer local topological features are found that are associated with the presence of the sharp front corners of the square cylinder and the slight geometrical asymmetry of the square cylinder set in the experiments. As shown in a zoomed-in view near the left side wall of the square cylinder in Fig. 5(a), the spiraling node N_4 and the saddle S_4 are revealed, which result from flow separation starting at the sharp front corner of the

square cylinder. As indicated in Fig. 5(b), the two additional singular points S_3 and N_3 occurs immediately downstream after the primary spiraling node N_1 on the left side of the cylinder. This combinations of $N_4 - S_4$ and $N_3 - S_3$ are also typical closed separation patterns.

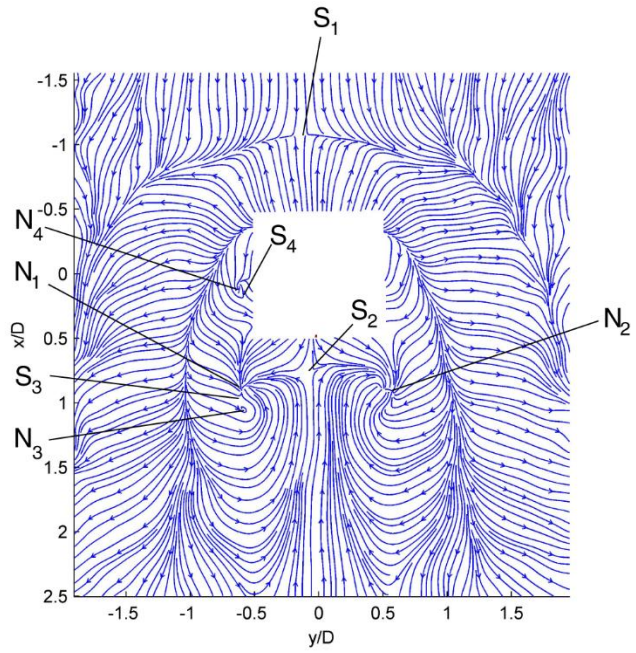

Figure 4. The global skin friction topology in the square junction flow: critical points.

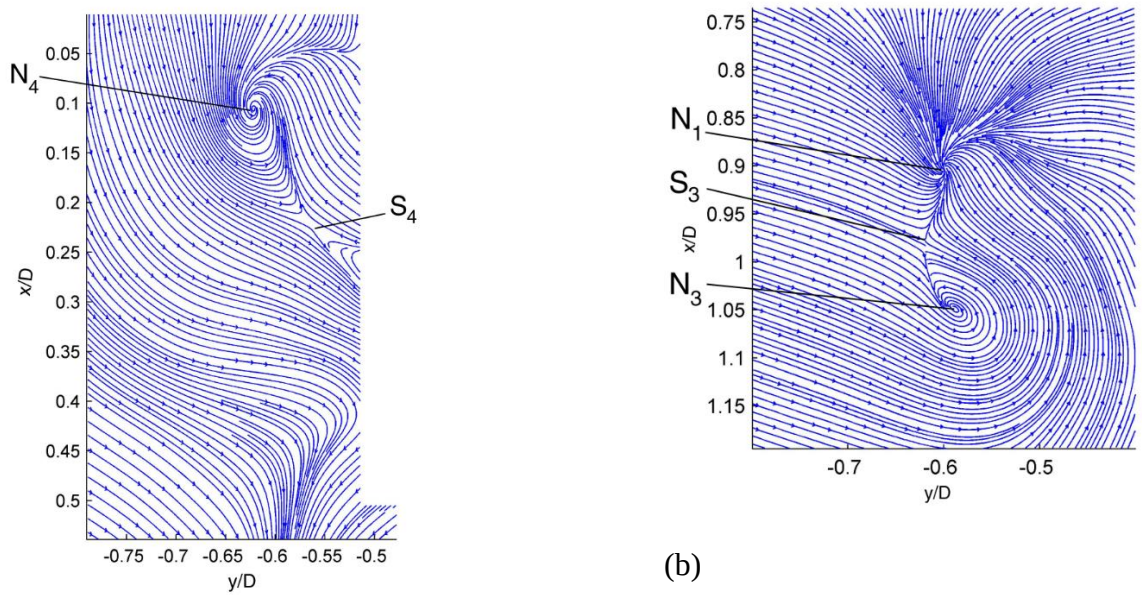

(a) (b)

Figure 5. The zoom-in view of the skin friction topology in the square junction flow: critical points.

(2) Availability

Operating system

Based on Matlab (R2007a, or later versions): Windows

Programming language

Matlab (R2007a, or later versions)

Additional system requirements

None

Dependencies

Several functions in Matlab image processing toolbox are required.

List of contributors

Tianshu Liu, Department of Mechanical and Aerospace Engineering, Western Michigan University

David M. Salazar, Department of Mechanical and Aerospace Engineering, Western Michigan University

Software location

Name: GitHub

Identifier: https://github.com/Tianshu-Liu/OpenOpticalFlow

License: MIT license

Data published: February 02, 2023

(3) Reuse Potential

Global skin friction diagnostics is of fundamental importance in the study of fluid mechanics in order to understand the physics of complex flows. The global luminescent oil-film (GLOF) method allows extraction of high-resolution skin friction fields from GLOF images obtained in various complex flows. The experimental setup for GLOF measurements is simple, and the GLOF images could be obtained by using inexpensive CCD and CMOS cameras under suitable illumination (such as UV light). The foundation of the GLOF method is well established based on the thin-oil-film equation projected onto the image plane. GLOF computation can be conducted in a PC with Matlab to extract skin friction fields at a spatial resolution of one vector per pixel. The GLOF method has been applied to complex separated flows. This open source program, "OpenSkinFrictionFromGLOF", allows users to adapt the GLOF method for their specific problems. Furthermore, "OpenSkinFrictionFromGLOF", can be integrated with Matlab for convenient image processing, data presentations, and data input/output. Besides GitHub, the

programs can be directly downloaded from the author's website https://wmich.edu/mechanical-aerospace/directory/liu.

References:

[1] Liu, T., Montefort, J., Woodiga, S., Merati, P. & Shen, L. 2008 Global luminescent oil film skin friction meter AIAA J 46(2), 476-485.

[2] Woodiga, S. & Liu, T. 2009 Skin friction fields on delta wings Exp Fluids 47, 897-911.

[3] Liu, T., Woodiga, S. & Ma, T. 2011 Skin friction topology in a region enclosed by penetrable boundary Exp Fluids 51, 1549-1562.

[4] Woodiga, S., Salasar, D. M., Wewengkang, P., Montefort, J. & Liu, T. 2018 Skin-friction topology on tail plate for tractor-trailer truck drag reduction J of Visualization 21, 1017-1029.

[5] Woodiga, S., Liu, T., Ramasamy, R. S. V. & Kode, S. 2015 Effects of pitch, yaw, and roll on delta wing skin friction topology. J Aero Eng 230(4)

[6] Husen, N., Liu, T. & Sullivan, J. P. 2018 The luminescent oil film flow tagging (LOFFT) skin friction meter applied to FAITH hill AIAA J 56(10), 3875-3886.

[7] Husen, N. 2017 Skin friction measurements using luminescent oil films, Ph.D. Thesis, Purdue University, West Lafayette, IN.

[8] Husen, N., Liu, T. & Sullivan, J. P. 2018 The ratioed image film thickness meter. Meas Sci Techno 29(6), 065301.

[9] Zhong, H., Woodiga, S., Wang, P., Shang, J., Cui, X., Wang, J. & Liu, T. 2015 Skin friction topology of wing-body junction flows Euro J Mech – B/Fluids 53, 55-67.

[10] Lee, T., Nonomura, T., Asai, T. & Liu, T. 2018 Linear-least-squares method for global luminescent oil-film skin-friction field analysis Rev Sci Instru 89(6), 065106.

[11] Tran, T. H., Amboa, T., Lee, T., Chen, L., Nonomura, T. & Asai, K. 2018 Effect of boattail angles on the flow pattern on an axisymmetric afterbody surface at low speed Exp Therm Fluid Sci 99, 324-335.

[12] Tran, T. H., Ambo, T., Lee, T., Ozawa, Y., Chen, L., Nonomura, T., & Asai, K. 2019 Effect of Reynolds number on flow behavior and pressure drag of axisymmetric conical boattails at low speeds Exp Fluids 60(3), 36.

[13] Liu, T. & Shen, L. 2008 Fluid flow and optical flow J Fluid Mech 614, 253-291.

[14] Wang, B., Cai, Z., Shen, L., & Liu, T. 2015 An analysis of physics-based optical flow method J Comp Appl Math 276, 62-80.

[15] Liu, T. 2017 OpenOpticalFlow: an open source program for extraction of velocity fields from flow visualization images J Open Res Software 5, 29.